Curvature-driven lipid sorting needs proximity to a demixing point and is aided by proteins

Benoit Sorre[a,b,1], Andrew Callan-Jones[a,1], Jean-Baptiste Manneville[b], Pierre Nassoy[a], Jean-François Joanny[a], Jacques Prost[a,c], Bruno Goud[b], and Patricia Bassereau[a,2]

[a]Unité Mixte de Recherche 168, Centre National de la Recherche Scientifique-Institut Curie-Université Pierre et Marie Curie, 26 rue d'Ulm, 75248 Paris Cedex 05, France; [b]Unité Mixte de Recherche 144, Centre National de la Recherche Scientifique-Institut Curie, 26 rue d'Ulm, 75248 Paris Cedex 05, France; and [c]Ecole Supérieure de Physique et de Chimie Industrielles, 10 rue Vauquelin, F-75231 Paris, France

Edited by Tom C. Lubensky, University of Pennsylvania, Philadelphia, PA, and approved February 13, 2009 (received for review November 6, 2008)

Sorting of lipids and proteins is a key process allowing eukaryotic cells to execute efficient and accurate intracellular transport and to maintain membrane homeostasis. It occurs during the formation of highly curved transport intermediates that shuttle between cell compartments. Protein sorting is reasonably well described, but lipid sorting is much less understood. Lipid sorting has been proposed to be mediated by a physical mechanism based on the coupling between membrane composition and high curvature of the transport intermediates. To test this hypothesis, we have performed a combination of fluorescence and force measurements on membrane tubes of controlled diameters pulled from giant unilamellar vesicles. A model based on membrane elasticity and nonideal solution theory has also been developed to explain our results. We quantitatively show, using 2 independent approaches, that a difference in lipid composition can build up between a curved and a noncurved membrane. Importantly, and consistent with our theory, lipid sorting occurs only if the system is close to a demixing point. Remarkably, this process is amplified when even a low fraction of lipids is clustered upon cholera toxin binding. This can be explained by the reduction of the entropic penalty of lipid sorting when some lipids are bound together by the toxin. Our results show that curvature-induced lipid sorting results from the collective behavior of lipids and is even amplified in the presence of lipid-clustering proteins. In addition, they suggest a generic mechanism by which proteins can facilitate lipid segregation in vivo.

cholera toxin | giant unilamellar vesicle | membrane curvature | membrane nanotube | optical tweezers

Lipids and proteins are not homogeneously distributed among cell membranes (1). How intracellular trafficking maintains the composition differences between the various membrane compartments of the cell is still poorly understood. In many cases, trafficking intermediates are tubular structures with radii typically in the range of 50 nm (2). It has been suggested that lipid sorting could be mediated by a physical mechanism based on the coupling between membrane composition and the high curvature of these intermediates (refs. 3–6; and see refs. 7–12 for theoretical papers) and on solid substrate topography (13). Added lipid or protein dyes have been shown to be sorted into or out of highly curved regions but without a systematic study of the influence of the underlying membrane composition on the sorting process (3, 14). It is crucial from a biological point of view to know whether the native membrane lipids themselves can be sorted by curvature and if so, whether or not the mechanism is robust for variable membrane compositions. In fact, a recent theoretical paper predicts a weak effect of curvature on membrane composition because of the overwhelming cost of mixing entropy, suggesting that curvature does not significantly contribute to sorting (15). In contrast, we demonstrate in the present work that cooperative behavior between lipids is a critical requirement to offset the entropic cost. As a result, the effectiveness of curvature-based sorting is highly sensitive to the proximity of the membrane composition to phase separation.

Membrane nanotubes pulled from multicomponent giant unilamellar vesicles (GUVs) by using micromanipulation techniques (16) are model systems perfectly suited to quantitatively validate the curvature-induced sorting hypothesis (17). Their radii can be controlled by setting the membrane tension by micropipette aspiration and can span from 10 to 200 nm. In GUVs made of a ternary mixture of, for instance, sphingomyelin (SM) or brain sphingomyelin (BSM), dioleylphosphatidylcholine (DOPC) and cholesterol (Chol), different liquid lipid phases are observed depending on the relative proportion of each lipid: a liquid-disordered (L_d) phase rich in DOPC or a liquid-ordered (L_o) phase rich in SM (18–20). Previous studies have shown that SM-rich membranes have a higher bending rigidity than DOPC-rich ones (14, 16, 19). If lowering the bending energy in a curved membrane by adjusting the lipid composition contributes to sorting, one would expect a relative depletion of SM in regions of high curvature. This effect has been calculated to be small in ideal lipid mixtures (15). However, lipid mixing in biological membranes is far from ideal (21, 22) and lipid–lipid interactions could potentially aid curvature-driven lipid sorting. Similarly, these interactions can be changed by the presence of proteins, such as toxins that are able to bind and cluster a fraction of lipids. Thus, whether membrane curvature is sufficient to cause lipid sorting in pure lipid mixtures as well as in biological membranes remains an important and open question.

In the present article, we have used 2 complementary approaches to measure lipid sorting as a function of membrane curvature: (*i*) confocal microscopy to measure sorting coefficients based on fluorescent lipid probes with different segregation behavior between L_o and L_d phases and (*ii*) optical tweezers to measure the force necessary to pull the tube. We have also developed a sorting model based on reduction of bending rigidity that includes lipid–lipid interactions. The model predicts the evolution of the sorting coefficient and the force on the tube as functions of curvature. We demonstrate that the proximity to a demixing point is essential for curvature-induced lipid sorting in an otherwise homogeneous lipid mixture. Our experimental observations are fully consistent with the theoretical model. In addition, we have studied, theoretically and experimentally, the consequences on lipid sorting of adding cholera toxin B-subunit

Author contributions: J.-F.J., J.P., B.G., and P.B. designed research; B.S. and A.C.-J. performed research; B.S. and P.N. contributed new reagents/analytic tools; B.S. and P.N. analyzed data; and B.S., A.C.-J., J.-B.M., J.-F.J., J.P., B.G., and P.B. wrote the paper.

The authors declare no conflict of interest.

This article is a PNAS Direct Submission.

[1]B.S. and A.C.-J. contributed equally to this work.

[2]To whom correspondence should be addressed at: Laboratoire PhysicoChimie, Centre de Recherche de l'Institut Curie, 26 Rue d'Ulm, F-75248 Paris, France. E-mail: patricia.bassereau@curie.fr.

This article contains supporting information online at www.pnas.org/cgi/content/full/0811243106/DCSupplemental.

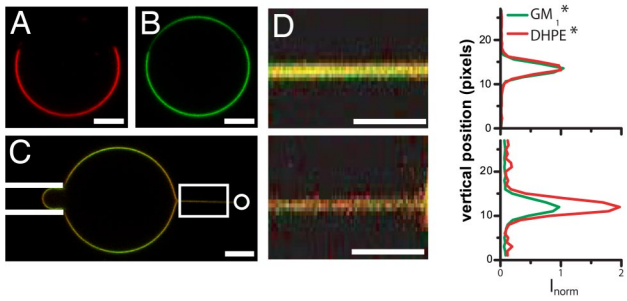

Fig. 1. Partitioning of fluorescent lipid dyes in GUVs and membrane nanotubes. (*A* and *B*) Confocal equatorial section of a 43:14:43 GUV showing the distribution of DHPE* [red (*A*)] and GM1* [green (*B*)] between 2 coexisting L_o and L_d phases. (*C*) Typical confocal image showing a tube pulled out of a 30:35:35 vesicle. A bead (not visible in fluorescence and represented by a white circle on the right side) trapped in the optical tweezers is bound to the vesicle. The vesicle is aspirated in a micropipette (left side, depicted with white lines) to set membrane tension and moved away from the trap to form a tube. Note that the intensity in the green channel is modulated along the vesicle contour because of the polarization of excitation light. This effect is taken into account in the data analysis. (*D*) Influence of membrane curvature on tube composition. (*Upper*) Confocal image (*Left*) of a membrane tube pulled out of a 30:35:35 GUV (zoom of the boxed region in *C*; the tube radius is 70 ± 10 nm) and corresponding tube length-averaged fluorescence profile for GM1* and DHPE* (*Right*). (*Lower*) Decreasing the radius of the above tube down to 20 ± 2 nm increases lipid sorting. DHPE* is approximately twice more concentrated than GM1* in the tube. For each dye, I_{norm} is the fluorescence intensity in the tube normalized by the fluorescence intensity in the vesicle and by the maximum of fluorescence of GM1* in the tube. (Scale bars, 5 μm.)

(CTxB), which binds and clusters 5 of the glycosphingolipid GM1 in the membrane. We first show that, regardless of the membrane composition, toxin-bound GM1 in the outer leaflet is depleted from the tube with increasing curvature. Unexpectedly, we also find that, in membranes close to a demixing point, lipid sorting is further amplified by toxin binding. This result indicates that lipid-clustering proteins may play an important role in curvature-induced sorting in biological membranes.

Results and Discussion

Sorting in Lipid Mixtures. To address the curvature-induced lipid sorting question, we have pulled membrane nanotubes of controlled radii from GUVs containing the ternary mixture BSM/Chol/DOPC. We have used 2 fluorescent lipids to detect lipid sorting: TexasRed-DHPE (DHPE*), which strongly segregates in the L_d phase (23, 24) [fluorescence ratio between L_d and L_o: $I_{L_D}/I_{L_O} = 65 \pm 15$ ($n = 9$ vesicles)] (Fig. 1*A*), and BodipyFL-GM1 (GM1*), which is equally distributed in the L_d and L_o phases ($I_{L_D}/I_{L_O} = 1.25 \pm 0.1, n = 9$ vesicles) (Fig. 1*B*). The incorporation of GM1 into GUV membrane was designed to allow binding of the B-subunit of cholera toxin. To address the question of curvature-induced sorting, we have built a setup combining confocal microscopy, optical tweezers, and micropipette aspiration [see supporting information (SI) Fig. S1]. By reducing confocal illumination, photobleaching was not significant, and photo-induced phase separation (14, 25) was not observed (see *SI Appendix* and Fig. S2). The membrane curvature was tuned by varying the tube radius, typically between 10 and 100 nm, through GUV aspiration (16). To detect sorting, (*i*) we compared the fluorescence of the markers in the membrane tube and in the GUV equatorial plane (Figs. 1 *C* and *D*) at steady state (Fig. S3), and (*ii*) we measured the force f exerted by the membrane nanotube on the trapped bead. In a single-component membrane, the force f_0 is given by (26)

$$f_0 = 2\pi\sqrt{2\kappa\sigma}, \qquad [1]$$

where σ is the membrane tension set by the pipette aspiration (16), and κ is the membrane bending rigidity. Departure of the square of the force, f^2, vs. σ from linearity reflects a difference between tube and mother vesicle compositions.

First, we established that no lipid sorting occurred in tubes pulled from homogenous L_d phase vesicles. We considered vesicles of pure DOPC (0:0:100), a mixture of DOPC and cholesterol (0:33:67), and a mixture containing BSM, cholesterol, and DOPC (17:33:50), all compositions being far from the phase separation limit (shown on the phase diagram in Fig. 2*D*). For these 3 compositions, containing 0.5% DHPE* and 1% GM1*, we have measured the sorting ratio defined as the ratio between the fluorescence intensities of DHPE (I_t^{DHPE}) and of GM1 (I_t^{GM1}) in the tube normalized by the same ratio in the vesicle (I_v^{DHPE}/I_v^{GM1}), corrected by a polarization factor (PCF) experimentally measured (for details, see *SI Appendix* and Table S2):

$$\text{Sorting} = \frac{1}{PCF} \times \left[\frac{I_t^{DHPE}/I_t^{GM1}}{I_v^{DHPE}/I_v^{GM1}} \right]. \qquad [2]$$

In the following, we plot our data as a function of $4\pi\sigma/f = C_r$, which is the reference tube curvature in the absence of sorting (26). For the above 3 compositions, the sorting ratio is equal to unity and is independent of C_r (Fig. 2*A*), showing no composition change.

In contrast, very different behavior is observed when more sphingomyelin is added, driving the mixture close to the phase boundary. For the 30:35:35 composition (see *Materials and Methods*), a monotonic increase in the sorting ratio is observed when curvature is increased. Sorting becomes significant for tube radii <30–40 nm (Figs. 1 *C* and *D* and 2*A*). Analysis of the fluorescent lipid distribution shows an enrichment of DHPE* in the tube, consistent with SM depletion, whereas the GM1* concentration remains constant as curvature increases (Fig. S4). Clearly, significant sorting of the fluorescent lipid markers can occur for compositions close to a phase boundary.

Additional evidence for lipid sorting can be obtained from the force f needed to hold the membrane nanotube. This force is related to the membrane composition and thus should also be sensitive to lipid sorting. Indeed, for the 3 compositions far from the phase-separation boundary, a linear variation of f^2 as a function of membrane tension σ is observed, as expected if the composition remains unchanged in the tube (Fig. 2*B* for 0:0:100 and Fig. S5 for 0:33:67 and 17:33:50). The slopes of these plots are proportional to the membrane bending rigidities (Table S1). In agreement with recent X-ray experiments (27), we observed that the bending rigidity of DOPC membranes is unchanged upon addition of 30% cholesterol. For the 30:35:35 composition, for which we have detected lipid sorting with fluorescence measurements, we observed a clear downward deviation from linear behavior; the force is lower than expected in the absence of sorting for the same vesicle composition (Fig. 2*B*). This deviation is independent of the presence of GM1* in the membrane, showing that the sorting effect on force is not a consequence of the labeling but only of this particular membrane composition (Fig. S9). This reduction in tube force provides direct evidence that a tube pulled from a vesicle with a composition close to phase separation can have a significantly different composition from the vesicle membrane.

Theoretically, the sorting of lipids between the tube and the vesicle is determined by a tradeoff between mixing and bending energies by excluding (enriching) those lipids with a tendency to form more (less) rigid bilayers. We developed a simple model that highlights the role of membrane tension, composition dependence of bending modulus, and mixing free energy based on an extension of the Helfrich membrane bending energy of the tube augmented by a Flory–Huggins mixing free energy for a

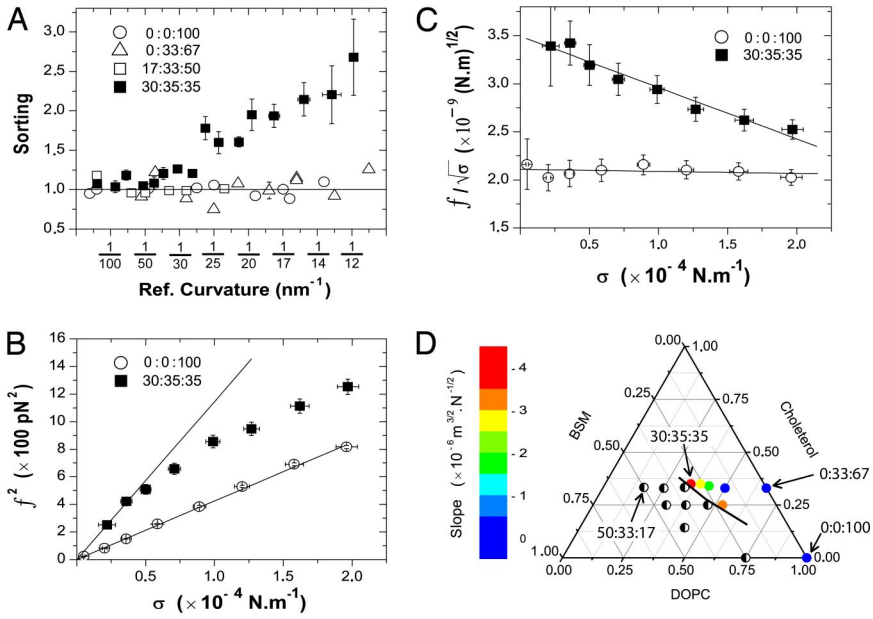

Fig. 2. Curvature-driven lipid sorting occurs only close to a phase separation. (*A*) Sorting of DHPE* to GM1* as a function of the reference curvature (Ref. curvature) for different lipid mixtures. For clarity, only 1 representative error bar is presented for the 0:0:100, 0:33:67, and 17:33:50 datasets. Data are binned over 4 points (n = 12 vesicles for 30:35:35; n = 10 for 0:0:100, 0:33:67, and n = 7 for 17:33:50; error bars represent standard error of the mean). The horizontal line (sorting = 1), a guide to the eye, corresponds to the absence of sorting. (*B*) Squared force f^2 vs. σ for typical 30:35:35 and 0:0:100 vesicles. A linear fit of f^2 vs. σ according to Eq. **1** gives $\kappa_v = 15 \pm 3\ k_BT$ for the 0:0:100 composition. For the 30:35:35 composition, a clear deviation from linear behavior is observed. The line corresponds to a linear fit of the first 3 points. Error bars correspond to experimental precision. (*C*) A linear fit to $f/\sqrt{\sigma}$ vs. σ according to Eq. **4** gives a slope of 5.1 10^{-6} m$^{3/2}$.N$^{-1/2}$ for 30:35:35 and 0.2 10^{-6} m$^{3/2}$.N$^{-1/2}$ for 0:0:100. From the extrapolation to $\sigma = 0$, we find $\kappa_v = 38\ k_BT$ for 30:35:35 and $\kappa_v = 15\ k_BT$ for 0:0:100. Error bars correspond to experimental precision. (*D*) Schematic phase diagram summarizing the evolution of sorting effect with membrane composition at T = 22 ± 1 °C. The color scale illustrates the average slopes extracted from the linear fits to $f/\sqrt{\sigma}$ versus σ plots (see Table S1). Half-filled circles, compositions showing phase separation; black line, phase boundary deduced from our observations (*SI Appendix*).

binary system (see *SI Appendix*). For small compositional differences between the tube and reservoir the free energy is

$$F = 2\pi RL\left[\frac{\kappa(\phi_t)}{2R^2} + \sigma + \frac{1}{2}f_v''(\phi_t - \phi_v)^2\right] - fL, \qquad [3]$$

where R is the tube radius; L is the tube length; $\kappa(\phi_t)$ is the bending modulus evaluated at the tube composition ϕ_t; and f_v'' is the second derivative of the mixing free energy (the inverse of the osmotic compressibility) with respect to area fraction ϕ, evaluated at the vesicle composition ϕ_v. Without any detailed knowledge of $\kappa(\phi_t)$ we can, however, for small sorting expand it to linear order about its value in the vesicle, $\kappa(\phi_t) \approx \kappa_v + \kappa_v'(\phi_t - \phi_v)$. Minimizing Eq. **3** with respect to ϕ_t gives the leading-order sorting $\Delta\phi = (\phi_t - \phi_v) = -\frac{\kappa_v'}{\kappa_v}\frac{\sigma}{f_v''}$. With $\frac{\kappa_v'}{\kappa_v} \approx 1.5$ (Table S1), a significant sorting requires a large osmotic compressibility, that is, in the range of accessible tensions, $f_v'' \ll k_BT\rho$, ρ being the lipid density and k_B Boltzmann's constant. This condition is verified only near continuous phase separations, as this is the case for the 30:35:35 mixture. Note that we have neglected any asymmetry between the 2 leaflets in our approach (28). The pulling force on the tube, obtained by minimizing Eq. **3** with respect to L, is:

$$f \approx 2\pi\sqrt{2\kappa_v\sigma}\left[1 - \frac{\sigma}{4f_v''}\left(\frac{\kappa_v'}{\kappa_v}\right)^2\right]; \qquad [4]$$

the second term in brackets is the leading correction to the pulling force due to sorting. Thus, a deviation from linearity of f vs. $\sqrt{\sigma}$ provides a quantitative measure of lipid sorting. Plotting $f/\sqrt{\sigma}$ vs. σ (Fig. 2*C*, Fig. S5, and Table S1), we observe a slope equal to zero for all tested compositions except for the composition 30:35:35, which demonstrates sorting in that mixture as expected from the above arguments. From Fig. 2*C*, we deduce $f_v''/kT\rho \approx 0.05$, consistent with this particular composition being close to phase separation.

To further test this hypothesis, we explored how lipid sorting varies as a function of the distance from a demixing point in the phase diagram (*SI Appendix*). When the SM/DOPC ratio is decreased at quasiconstant cholesterol fraction (26:35:39 and 23:34:43 mixtures), we observe that sorting becomes weaker as we move away from the phase boundary. Both the sorting coefficient and the magnitude of the slope of $f/\sqrt{\sigma}$ vs. σ decreases (Fig. S6*a* and Table S1). Furthermore, another lipid composition at the phase limit (22:25:53) gives a sorting coefficient of the same order as the one obtained for the 30:35:35 mixture (Table S1 and Fig. S6*b*). The average slopes of $f/\sqrt{\sigma}$ versus σ obtained with various lipid compositions are summarized in Fig. 2*D*. Altogether, the above data indicate that lipid sorting requires proximity to a demixing point.

Effect of Toxin Binding on Lipid Sorting. Several groups have shown (22, 29, 30) that the pentameric B-subunit of the cholera-toxin (CTxB), binding 5 GM1 lipids (31), is able to induce phase separation in otherwise uniformly mixed membranes (Fig. S7). This suggests that, when lipids are bound to a protein, the osmotic compressibility of the lipid mixture can effectively rise. The influence of CTxB on curvature-induced lipid sorting is, however, not known and has not been investigated both theoretically and experimentally. We thus repeated the fluorescence and force experiments described above with GUVs of the same lipid compositions but now in the presence of CTxB in solution. We checked that the amount of CTxB used was low enough to

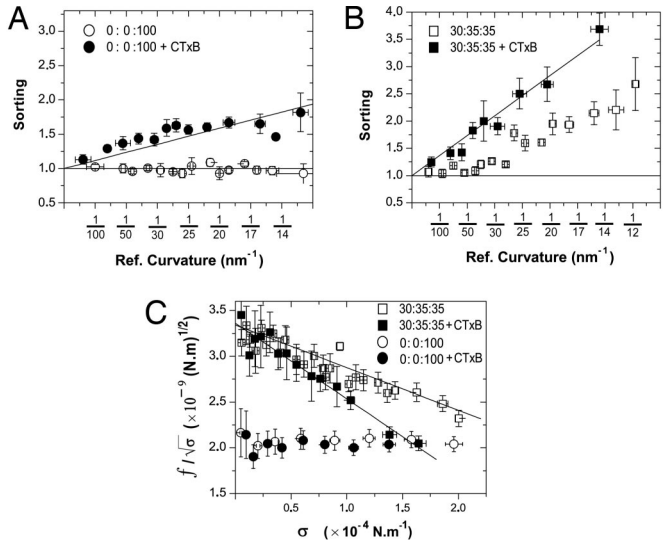

Fig. 3. Cholera toxin B-subunit (CTxB) binding to GM1 enhances lipid sorting. (*A* and *B*) Sorting ratio for DHPE* to GM1* as a function of the reference curvature (Ref. curvature) for 0:0:100 vesicles (*A*) and for 30:35:35 vesicles (*B*) with (filled symbols) and without (open symbols) CTxB in solution. Linear fits in the presence of CTxB give $(11.7 \times C_r + 1)$ for the 0:0:100 composition and $(37 \times C_r + 1)$ for the 30:35:35 composition, with the reference curvature C_r in nm^{-1}. Data are binned over 4 points (for 0:0:100, $n = 9$ vesicles with CTxB and $n = 10$ without; for 30:35:35, $n = 8$ vesicles with CTxB and $n = 12$ without; error bars represent the standard error of the mean). The horizontal line (sorting = 1), a guide to the eye, corresponds to the absence of sorting. (*C*) Effect of CTxB binding on the tube force. The force is plotted as $f/\sqrt{\sigma}$ vs. σ following Eq. **4**. Data for the 30:35:35 membranes are binned over 4 points ($n = 8$ vesicles with CTxB and $n = 12$ without; error bars represent the standard error of the mean). Linear fits give: $(-8.3 \times 10^{-6} \times \sigma + 3.4 \times 10^{-9})$ and $(-4.5 \times 10^{-6} \times \sigma + 3.3 \times 10^{-9})$ for the 30:35:35 composition with and without CTxB, respectively.

avoid phase separation in the ternary GUVs, in particular for the 30:35:35 composition. Interestingly, sorting was found to be significantly amplified in the vicinity of a phase separation in the presence of CTxB. For the 30:35:35 mixture, the sorting ratio of DHPE* to GM1* is increased by CTxB binding (Fig. 3*B*). This could reveal either the coupling of CTxB concentration to curvature or the enhancement of lipid sorting by CTxB binding. As a control, we measured the sorting ratio of DHPE* to GM1* in pure DOPC (0:0:100) and in mixtures far from phase separation (0:33:67 and 17:33:50) in the presence of CTxB. These experiments show a GM1* depletion from the tube (Fig. 3*A* and Figs. S4 and S8). Importantly, GM1* depletion occurs for all tested compositions. This is consistent with experimental evidence showing that CTxB bound to the external leaflet of a GUV induces inward rather than outward bending deformation (personal communication), which suggests a physical mechanism by which CTxB/GM1* complexes are depleted from tubes. GM1 depletion also corresponds to a CTxB depletion from the tube, as confirmed with experiments using fluorescent CTxB (CTxB*) binding to nonfluorescent GM1 (Fig. S4*e*). Interestingly, because of CTxB binding, GM1 is asymmetrically sorted. On the one hand, the sorting coefficient is <2 even at high curvature (Fig. S8) when GM1* is used, indicating that the inner leaflet remains unaffected by CTxB binding. On the other hand, a sorting coefficient >2 is obtained when fluorescent CTxB* is used in the same conditions (Fig. S8*b*). Compared with fluorescence experiments, force measurements do not exhibit any signature of lipid sorting for the 0:0:100, 0:33:67, and 17:33:50 mixtures (Fig. 3*C* for 0:0:100 and Fig. S5 for 0:33:67 and 17:33:50). The measurement of the sorting ratio is thus a measure of CTxB exclusion only. Note that, in principle, even in the absence of lipid sorting, the force should depend on bound CTxB concentration, because of the possible CTxB dependence of the bending modulus and because of its preferred curvature (*SI Appendix*). Our experiments show that this effect is negligible, because for all of the mixtures we investigated, $f/\sqrt{\sigma}$ at vanishing tension does not depend on the presence of CTxB (Fig. 3*C* and Table S1). Force measurement on the 30:35:35 mixture, however, demonstrate a strong increase in sorting, reflected by a doubling of the slope of $f/\sqrt{\sigma}$ vs. σ from $-(4.6 \pm 1) \times 10^{-6}$ m$^{3/2}$·N$^{-1/2}$ in the absence of toxin to $-(8.0 \pm 2) \times 10^{-6}$ m$^{3/2}$·N$^{-1/2}$ in its presence (Fig. 3*C* and Table S1). Note that the sorting is so effective that at large curvatures, the force approaches the value measured for 0:0:100 (Fig. 3*C*) or 0:33:67 mixture (Fig. S5*b*), showing that the tube is completely depleted of SM.

Fig. 3 *A* and *B* and Fig. S8 indicate that, except for the 30:35:35 mixture, the exclusion of CTxB/GM1* complex is independent of vesicle composition. We rationalize these results by minimizing a free energy that includes contributions from mixing, bending and coupling between curvature and protein concentration (*SI Appendix*). We find that the exclusion of protein complex, $\Delta\phi$, increases linearly with tube curvature or, correct to this order, with $\sqrt{\sigma}$ and with, x, the number of lipids bound and clustered by a single toxin, which for CTxB is equal to 5 (*SI Appendix*). We further find that in the small ϕ_v limit, the fluorescence ratio is equal to $1 - \Delta\phi/2\phi_v$, the factor of 2 reflecting that GM1 on the inner leaflet is unaffected by curvature (*SI Appendix*). The fluorescence ratios in Fig. 3*A* and Fig. S8 increase linearly with curvature, in agreement with our prediction. One expects that the sole effect of coupling between curvature and CTxB concentration on the tube force is a downward shift in the bending modulus, proportional to the concentration of bound protein (8). The fact that the forces for 0:0:100 in Fig. 3*C* and in Fig. S5 for 0:33:67 and 17:33:50 show no difference whether CTxB is bound or not can be explained in view of the very low concentration of GM1/CTxB complex in the membrane and of the proportionality of the force correction to the square of the coupling term, which is small in our system (*SI Appendix*).

The presence of bound protein does, however, have a measurable effect on the force behavior for the 30:35:35 mixture (*SI Appendix*). We propose that the addition of CTxB has an amplifying effect on lipid sorting near a demixing transition. The physical reason for this is that, linking the GM1* lipids in groups reduces the translational entropy of the lipids in the tube plus vesicle system. In other words, the balance between mixing entropy and enthalpy (lipid–lipid interactions) is shifted in favor of enthalpy, thus reducing the penalty for sorting. A simple calculation shows that the addition of CTxB leads to a fractional decrease of the inverse osmotic compressibility for sorting proportional to $\phi_{GM1}(x-1)/f^{''}_{(0)}$, where ϕ_{GM1} is the area fraction of GM1* in the vesicle, equal to 1%, x is the number of GM1* lipids bound to a single CTxB, equal to a maximum of 5, and $f^{''}_{(0)}$ is the inverse osmotic compressibility in the absence of CTxB (see *SI Appendix*). Therefore, even for a small concentration of GM1*, the relative effect on sorting can be significant if $f^{''}_{(0)}$ is small, that is, near to the demixing point of the CTxB-free system.

Conclusion

We have shown here that lipid sorting can occur in lipid membranes by the formation of curved membrane structures without the help of any cellular protein machinery. Our first conclusion of this work is that lipid sorting is effective only near phase separation. This result seems to have been ignored so far in theoretical models. It cannot be obtained from a geometrical, molecular description and requires the consideration of the collective behavior of the lipids. There is strong evidence that biological plasma membranes and maybe some intracellular membranes are close to phase separation (1, 22, 23), enhancing

their sensitivity to composition fluctuations. We found that the sorting of specific lipids can also be affected, independently of the membrane composition, by proteins, such as CTxB, that bind and cluster those lipids. Our last conclusion is that CTxB drives the lipid mixture closer to phase separation. This amplifies curvature-driven lipid sorting. This generic mechanism can be at work in cells for many proteins involved in the formation of transport intermediates.

Materials and Methods

GUVs. GUVs made of mixtures of brain sphingomyelin (BSM), cholesterol (Chol), and dioleylphosphatidylcholine (DOPC) were grown by using the electroformation technique (32) at 60 °C in 300 mOsm sucrose solution. BODIPY $_{FL}$C5-GM1 (GM1*) was initially added at 1% (molar fraction, n/n) to these lipid mixtures and TexasRed -DHPE (DHPE*) at 0.5% (molar fraction, n/n). To allow adhesion between the membrane and the streptavidin-coated beads holding the tube in the trap, 0.03% (n/n) of DSPE-PEG(2000)-Biotin was added to the lipid mixture. Lipid compositions are expressed as mole fractions of BSM/Chol/DOPC. The 30:35:35 mixture corresponds to the closest composition to the phase boundary where 100% of the GUVs exhibit an homogeneous fluorescence at 35% cholesterol. When used, CTxB was added at a concentration of 50 nM.

Force and Tension Measurements, Tube Radius Calculation. The force f exerted by the tube was deduced from the displacement $x - x_0$ of the bead from its equilibrium position x_0 in the optical trap by using the linear relationship $f = k(x - x_0)$, where k is the trap stiffness. The bead position was measured off-line by video tracking (16). k was determined by the viscous drag method (33). The membrane tension σ was determined by using $\sigma = (\Delta P \cdot R_{pip})/2(1 - R_{pip}/R_{ves})$ where R_{pip} is the pipette radius, R_{ves} the vesicle radius, and ΔP the difference of hydrostatic pressure caused by the vertical displacement of the water reservoir linked to the pipette (34). For each data point, the reference tube curvature C_r in the absence of sorting was calculated from the independent measurements of f and σ by using $C_r = 1/r = 4\pi\sigma/f$ (26).

ACKNOWLEDGMENTS. We thank L. Berland, A. Roux, E. Ambroggio, L. Johannès, and J. Derganc for stimulating discussions; D. van Effenterre for help with the initial experiments; G. Toombes for a constructive reading of the manuscript and for inspiring discussions; and B. Lemaire for the mechanics of the experimental set-up. This work was supported by: European Commission (NoE SoftComp), the Curie Institute (PIC Physique du Vivant), and the Human Frontier Science Program Organisation. The groups belong to the French research consortium ''CellTiss.'' B.S. is supported by a grant from the Direction Générale pour l'Armement and from the Centre National de la Recherche Scientifique; A.C.-J holds a postdoctoral fellowship from SoftComp and the Association pour la Recherche Contre le Cancer.

1. van Meer G, Voelker DR, Feigenson GW (2008) Membrane lipids: Where they are and how they behave. *Nat Rev Mol Cell Biol* 9:112–124.
2. Alberts B, et al. (2002) *Molecular Cell Biology of the Cell* (Garland Science), 4th Ed.
3. Mukherjee S, Soe TT, Maxfield FR (1999) Endocytic sorting of lipid analogues differing solely in the chemistry of their hydrophobic tails. *J Cell Biol* 144:1271–1284.
4. Mukherjee S, Maxfield FR (2000) Role of membrane organization and membrane domains in endocytic lipid trafficking. *Traffic* 1:203–211.
5. van Meer G, Lisman Q (2002) Sphingolipid transport: Rafts and translocators. *J Biol Chem* 277:25855–25858.
6. van Meer G, Sprong H (2004) Membrane lipids and vesicular traffic. *Curr Opin Cell Biol* 16:373–378.
7. Markin VS (1981) Lateral organization of membranes and cell shapes. *Biophys J* 36:1–19.
8. Leibler S (1986) Curvature instability in membranes. *J Phys* 47:507–516.
9. Seifert U (1993) Curvature-induced lateral phase segregation in two-component vesicles. *Phys Rev Lett* 70:1335–1338.
10. Chen C-M, Higgs PG, Mackintosh FC (1997) Theory of fission for two-component lipid vesicles. *Phys Rev Lett* 79:1579–1582.
11. Derényi I, et al. (2007) Membrane nanotubes. Controlled nanoscale motion. *Lecture Notes in Physics* (Springer, Berlin), Vol 711, pp 141–159.
12. Jiang H, Powers TR (2008) Curvature-driven lipid sorting in a membrane tubule. *Phys Rev Lett* 101:018103.
13. Yoon T-Y, et al. (2006) Topographic control of lipid-raft reconstitution in model membranes. *Nat Mat* 5:281–285.
14. Roux A, et al. (2005) Role of curvature and phase transition in lipid sorting and fission of membrane tubules. *EMBO J* 24:1537–1545.
15. Derganc J (2007) Curvature-driven lateral segregation of membrane constituents in golgi cisternae. *Phys Biol* 4:317–324.
16. Cuvelier D, Derényi I, Bassereau P, Nassoy P (2005) Coalescence of membrane tethers: Experiments, analysis and applications. *Biophys J* 88:2714–2726.
17. Sens P, Johannes L, Bassereau P (2008) Biophysical approaches to protein-induced membrane deformations in trafficking. *Curr Opin Cell Biol* 20:476–482.
18. Dietrich C, et al. (2001) Lipid rafts reconstituted in model membranes. *Biophys J* 80:1417–1428.
19. Baumgart T, Hess ST, Webb WW (2003) Imaging coexisting fluid domains in biomembrane models coupling curvature and line tension. *Nature* 425:821–824.
20. Kahya N, Scherfeld D, Bacia K, Poolman B, Schwille P (2003) Probing lipid mobility of raft-exhibiting model membranes by fluorescence correlation spectroscopy. *J Biol Chem* 278:28109–28115.
21. Baumgart T, et al. (2007) Large-scale fluid/fluid phase separation of proteins and lipids in giant plasma membrane vesicles. *Proc Natl Acad Sci USA* 104:3165–3170.
22. Lingwood D, Ries J, Schwille P, Simons K (2008) Plasma membranes are poised for activation of raft phase coalescence at physiological temperature. *Proc Natl Acad Sci USA* 105:10005–10010.
23. Baumgart T, Hunt G, Farkas ER, Webb WW, Feigenson GW (2007) Fluorescence probe partitioning between l_o/l_d phases in lipid membranes. *Biochim Biophys Acta* 1768:2182–2194.
24. Veatch SL, Keller SL (2003) A closer look at the canonical 'raft mixture' in model membrane studies. *Biophys J* 84:725–726.
25. Yuan J, Hira SM, Strouse GF, Hirst LS (2008) Lipid bilayer discs and banded tubules: Photoinduced lipid sorting in ternary mixtures. *J Am Chem Soc* 130:2067–2072.
26. Derényi I, Jülicher F, Prost J (2002) Formation and interaction of membrane tubes. *Phys Rev Lett* 88:238101.
27. Pan J, Mills TT, Tristram-Nagle S, Nagle JF (2008) Cholesterol perturbs lipid bilayers nonuniversally. *Phys Rev Lett* 100:198103–198104.
28. Svetina S, Zeks B, Waugh RE, Raphael RM (1998) Theoretical analysis of the effect of the transbilayer movement of phospholipid molecules on the dynamic behavior of a microtube pulled out of an aspirated vesicle. *Eur Biophys J* 27:197–209.
29. Bacia K, Schwille P, Kurzchalia T (2005) Sterol structure determines the separation of phases and the curvature of the liquid-ordered phase in model membranes. *Proc Natl Acad Sci USA* 102:3272–3277.
30. Hammond AT, et al. (2005) Crosslinking a lipid raft component triggers liquid ordered-liquid disordered phase separation in model plasma membranes. *Proc Natl Acad Sci USA* 102:6320–6325.
31. Ribi HO, Ludwig DS, Mercer KL, Schoolnik GK, Kornberg RD (1988) Three-dimensional structure of cholera toxin penetrating a lipid membrane. *Science* 239:1272–1276.
32. Mathivet L, Cribier S, Devaux PF (1996) Shape change and physical properties of giant phospholipid vesicles prepared in the presence of an ac electric field. *Biophys J* 70:1112–1121.
33. Neuman KC, Block SM (2004) Optical trapping. *Rev Sci Instrum* 75:2787–2809.
34. Kwok R, Evans E (1981) Thermoelasticity of large lecithin bilayer vesicles. *Biophys J* 35:637–652.